ACS OMEGA

Open Access

http://pubs.acs.org/journal/acsodf

Article

In Situ Temperature-Dependent Properties of Metal−Organic Framework ZIF-Coated ZnO Hybrid Structures: Structural and Advanced Spectroscopic Insights

Rajat Nagpal, Masaya Sugihara, Cristian Lupan, Nicolae Magariu, Tim Tjardts, Nahomy Meling Lizarde, Thomas Strunskus, Justin Jetter, Haoyi Qiu, Barnika Chakraborty, Tayebeh Ameri, Eckhard Quandt, Rainer Adelung,* Rob Ameloot, and Oleg Lupan*

Cite This: *ACS Omega* 2026, 11, 29178−29201

Read Online

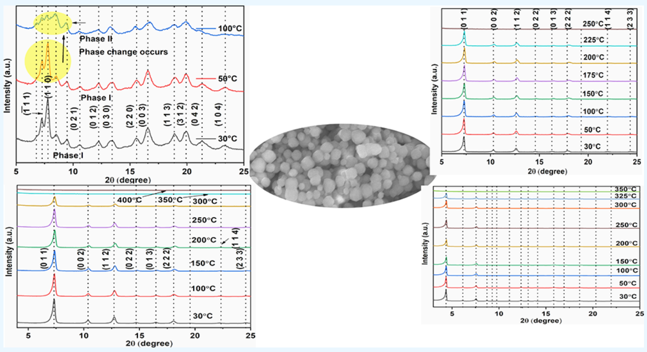

ABSTRACT: Advancements in material design, specifically the development of hybrids combining metal oxides (MO_x) and zeolitic imidazolate frameworks (MOF/ZIFs), have revolutionized modern materials science by employing their synergistic effects and creating the hybrid interface MOF/MO_x. This work systematically examines the structural evolution, defect engineering, and thermal stability of zeolitic imidazolate framework (ZIF-7, ZIF-8, ZIF-67, and ZIF-71)-coated ZnO and Cd-doped ZnO columnar structures. Comprehensive characterization was performed on all four studied ZIFs, including scanning electron microscopy revealing dodecahedral morphology of ZIF particles, and *in situ* temperature-dependent X-ray diffraction showing smaller coherently scattering regions compared to the sizes of the particles. SEM images indicate that these particles are polycrystalline and show a large contribution of surface-related domains. Thermolysis behavior and bond energy analysis reveal the role of Co−N bonds in thermal degradation of ZIF-67 at 250 °C compared to Zn−N bond of ZIF-8, which degrades at 325 °C, although Co−N has a higher bond energy compared to Zn−N, attributed to unsaturated coordination of Co with N, which leads to easy oxygenation of a Co−N bond. In ZIF-71 and ZIF-8, peak shifts are observed at higher angles by increasing the temperature, which would point to a negative thermal expansion. Using current−voltage characteristics, an inverted hysteresis was observed by employing forward and reverse voltage sweep, which may be characterized as capacitive hysteresis attributed to charge traps that slow down the return path. Gas-sensing studies revealed functional implications that ZIF-67-coated ZnO exhibited selective VOC sensing at 250 °C and enhanced hydrogen sensing at 300 °C, with structure−property correlations elucidated through defect analysis. Other hybrid materials, such as ZIF-7-coated ZnO, ZIF-8-coated ZnO, and ZIF-71-coated ZnO, elucidate better hydrogen, n-butanol, and 2-propanol sensing compared to ethanol and acetone. Our findings highlight the critical role of ZIF type and Cd doping in tuning the structural, thermal, and functional properties of ZnO-based composites, offering new perspectives for the rational design of advanced sensing materials based on the hybrid interface MOF/MO_x.

Received: March 17, 2026
Revised: April 15, 2026
Accepted: April 24, 2026
Published: May 4, 2026

https://doi.org/10.1021/acsomega.6c02238
ACS Omega 2026, 11, 29178−29201

■ REFERENCES

(1) Nagpal, Rajat; Sugihara, M.; Magariu, N.; Tjardts, T.; Meling-Lizarde, N.; Strunskus, T.; Ameri, T.; Ameloot, R.; Adelung, R.; Lupan, O. Humidity-Tolerant Selective Sensing of Hydrogen and n-Butanol Using ZIF-8 Coated CuO:Al Film. *Mater. Chem. Front.* **2025**, *9* (23), 3425−3442.

(2) Ji, J.; Lou, W.; Shen, P. Modular Design in Metal-Organic Frameworks for Oxygen Evolution Reaction. *Int. J. Hydrogen Energy* **2022**, *47* (93), 39443−39469.

(3) Li, D.; Yadav, A.; Zhou, H.; Roy, K.; Thanasekaran, P.; Lee, C. Advances and Applications of Metal-Organic Frameworks (MOFs) in Emerging Technologies: A Comprehensive Review. *Global Challenges* **2024**, *8* (2), No. 2300244.

(4) Xu, B.; Mei, Y.; Xiao, Z.; Kang, Z.; Wang, R.; Sun, D. Monitoring Thermally Induced Structural Deformation and Framework Decomposition of ZIF-8 through in Situ Temperature Dependent Measurements. *Phys. Chem. Chem. Phys.* **2017**, *19* (40), 27178−27183.

(5) Chaplais, G.; Fraux, G.; Paillaud, J.-L.; Marichal, C.; Nouali, H.; Fuchs, A. H.; Coudert, F.-X.; Patarin, J. Impacts of the Imidazolate Linker Substitution (CH3, Cl, or Br) on the Structural and Adsorptive Properties of ZIF-8. *J. Phys. Chem. C* **2018**, *122* (47), 26945−26955.

(6) Zhao, P.; Bennett, T. D.; Casati, N. P. M.; Lampronti, G. I.; Moggach, S. A.; Redfern, S. A. T. Pressure-Induced Oversaturation and Phase Transition in Zeolitic Imidazolate Frameworks with Remarkable Mechanical Stability. *Dalton Trans.* **2015**, *44* (10), 4498−4503.

(7) Wu, C.; Xie, D.; Mei, Y.; Xiu, Z.; Poduska, K. M.; Li, D.; Xu, B.; Sun, D. Unveiling the Thermolysis Natures of ZIF-8 and ZIF-67 by Employing in Situ Structural Characterization Studies. *Phys. Chem. Chem. Phys.* **2019**, *21* (32), 17571−17577.

(8) Gadipelli, S.; Travis, W.; Zhou, W.; Guo, Z. A Thermally Derived and Optimized Structure from ZIF-8 with Giant Enhancement in CO2 Uptake. *Energy Environ. Sci.* **2014**, *7* (7), 2232−2238.

(9) Nagpal, R.; Lupan, C.; Buzdugan, A.; Ghenea, V.; Lupan, O. Effect of Pd Functionalization on Optical and Hydrogen Sensing Properties of ZnO: Eu Films. *Optik (Stuttg)* **2025**, *325*, No. 172247.

(10) Zhang, Y.; Li, X.; He, Q.; Hameed, M.; Briscoe, J. Hybrid Energy Harvester Integrating ZnO Piezoelectric Nanogenerator with Perovskite Solar Cell Demonstrating the Piezo-Phototronic Effect. *Nano Energy* **2025**, *141*, No. 111120.

(11) Bayan, S.; Mohanta, D. Significant Fowler−Nordheim Tunneling across ZnO − Nanorod Based Nanojunctions for Nanoelectronic Device Applications. *Curr. Appl. Phys.* **2013**, *13* (4), 705−709.

(12) Nagpal, Rajat; Lupan, C.; Bîrnaz, A.; Sereacov, A.; Greve, E.; Gronenberg, M.; Siebert, L.; Adelung, R.; Lupan, O. Multifunctional Three-in-One Sensor on t-ZnO for Ultraviolet and VOC Sensing for Bioengineering Applications. *Biosensors* **2024**, *14* (6), 293.

(13) Lupan, O.; Santos-Carballal, D.; Magariu, N.; Mishra, A. K.; Ababii, N.; Krüger, H.; Wolff, N.; Vahl, A.; Bodduluri, M. T.; Kohlmann, N.; Kienle, L.; Adelung, R.; de Leeuw, N. H.; Hansen, S. Al_2O_3/ZnO Heterostructure-Based Sensors for Volatile Organic Compounds in Safety Applications. *ACS Appl. Mater. Interfaces* **2022**, *14* (25), 29331−29344.

(14) Santos-Carballal, D.; Lupan, O.; Magariu, N.; Ababii, N.; Krüger, H.; Bodduluri, M. T.; de Leeuw, N. H.; Hansen, S.; Adelung, R. Al_2O_3/ZnO Composite-Based Sensors for Battery Safety Applications: An Experimental and Theoretical Investigation. *Nano Energy* **2023**, *109*, No. 108301.

(15) Shin, J.; Choi, S.-W.; Kim, C.; Park, J.; Roh, J. W.; Hwang, J. Y.; Mirzaei, A.; Jin, C.; Choi, M. S. Characterization and H_2S Gas Sensing

Characteristics of Au-Decorated ZnO Nanorods Prepared by a Two-Step Wet Method. *J. Alloys Compd.* **2025**, *1021*, No. 179655.

(16) Wang, Z. L. Nanostructures of Zinc Oxide. *Mater. Today* **2004**, *7* (6), 26−33.

(17) Wadatkar, A. S.; Kharat, P. B.; Ambhore, A. V.; Onkar, S. G. Low-Cost Fabrication of Cu Doped ZnO (Zn0.95Cu0.05O) Film for Enhanced Gas Sensing Applications. *J. Phys. Conf. Ser.* **2020**, *1644* (1), No. 12059.

(18) Nam, B.; Ko, T.-K.; Hyun, S.-K.; Lee, C. Sensitivities of a 6:4 (by Molar Ratio) ZnO/WO_3 Composite Nanoparticle Sensor to Reducing and Oxidizing Gases. *Appl. Surf. Sci.* **2020**, *504*, No. 144104.

(19) Lupan, O.; Schröder, S.; Abdollahifar, M.; Magariu, N.; Offermann, J.; Schwäke, L.; Brinza, L.; Zimoch, L.; Tugulea, V.; Strunskus, T.; Adelung, R.Polymer-Coated Cd-Doped ZnO Nanostructures for Dual Sensing of Volatile Organic Compounds and Battery Vapours. In *7th International Conference on Nanotechnologies and Biomedical Engineering*; Springer Nature Switzerland: Cham, Sontea, V.; Tiginyanu, I.; Railean, S. Ed.; 2025; pp 284−300.

(20) Chiriac, M.; Minaee, H.; Rehder, S.; Ababii, N.; Magariu, N.; Sereacov, A.; Adejube, B.; Vahl, A.; Adelung, R.; Ameri, T.; Terraschke, H.Performance of Ag_2S/ZnO Nanostructures in Radiation Monitoring. In *7th International Conference on Nanotechnologies and Biomedical Engineering*; Springer Nature Switzerland: Cham, Sontea, V.; Tiginyanu, I.; Railean, S.Ed.; 2025; pp 237−246.

(21) Li, G.-R.; Zhao, W.-X.; Bu, Q.; Tong, Y.-X. A Novel Electrochemical Deposition Route for the Preparation of $Zn_{1-x}Cd_xO$ Nanorods with Controllable Optical Properties. *Electrochem. commun.* **2009**, *11* (2), 282−285.

(22) Jule, L. T.; Dejene, F. B.; Ali, A. G.; Roro, K. T.; Hegazy, A.; Allam, N. K.; El Shenawy, E. Wide Visible Emission and Narrowing Band Gap in Cd-Doped ZnO Nanopowders Synthesized via Sol-Gel Route. *J. Alloys Compd.* **2016**, *687*, 920−926.

(23) Yao, M. S.; Cao, L. A.; Tang, Y. X.; Wang, G. E.; Liu, R. H.; Kumar, P. N.; Wu, G. D.; Deng, W. H.; Hong, W. J.; Xu, G. Gas Transport Regulation in a MO/MOF Interface for Enhanced Selective Gas Detection. *J. Mater. Chem. A* **2019**, *7* (31), 18397−18403.

(24) Huang, B.; Zeng, W.; Li, Y. Synthesis of ZIF-8 Coating on ZnO Nanorods for Enhanced Gas-Sensing Performance. *Chemosensors* **2022**, *10* (8), 297.

(25) Ren, G.; Li, Z.; Yang, W.; Faheem, M.; Xing, J.; Zou, X.; Pan, Q.; Zhu, G.; Du, Y. ZnO@ZIF-8 Core-Shell Microspheres for Improved Ethanol Gas Sensing. *Sens. Actuators, B* **2019**, *284*, 421−427.

(26) Lin, D.; Duan, P.; Yang, W.; Liu, Y.; Pan, Q. Facile Controlled Synthesis of Core−Shell/Yolk−Shell/Hollow ZIF-67@Co-LDH/SiO_2via a Self-Template Method. *Inorg. Chem. Front.* **2020**, *7* (8), 1643−1650.

(27) Zhou, T.; Sang, Y.; Wang, X.; Wu, C.; Zeng, D.; Xie, C. Pore Size Dependent Gas-Sensing Selectivity Based on ZnO@ZIF Nanorod Arrays. *Sens. Actuators, B* **2018**, *258*, 1099−1106.

(28) Zhang, K.; Zhang, L.; Jiang, J. Adsorption of C1−C4 Alcohols in Zeolitic Imidazolate Framework-8: Effects of Force Fields, Atomic Charges, and Framework Flexibility. *J. Phys. Chem. C* **2013**, *117* (48), 25628−25635.

(29) Matatagui, D.; Sainz-Vidal, A.; Gràcia, I.; Figueras, E.; Cané, C.; Saniger, J. M. Chemoresistive Gas Sensor Based on ZIF-8/ZIF-67 Nanocrystals. *Sens. Actuators, B* **2018**, *274*, 601−608.

(30) Keyvanloo, Z.; Nakhaei Pour, A.; Moosavi, F. Adsorption and Diffusion of the $H_2/CO_2/CO$/MeOH/EtOH Mixture into the ZIF-7 Using Molecular Simulation. *J. Mol. Graph. Model.* **2022**, *116*, No. 108275.

(31) Ma, C.; Zhou, T.; Yang, H.; Su, H.; Wang, X.; Wu, Q.; Guo, X.; Zeng, D. High Selectivity and Response H_2 Sensors Based on ZnO@ZIF-71@Ag Nanorod Arrays. *Ceram. Int.* **2023**, *49* (12), 19728−19736.

(32) Aleem, M.; Zhou, Y.; Deswal, S.; Lee, B.; Misra, V. Novel Sequential Detection of NO_2 and C_2H_5OH in SnO_2MEMS Arrays for Enhanced Selectivity in E-Nose Applications. *Chemosensors* **2024**, *12* (12), 268.

(33) More, M. S.; Bodkhe, G. A.; Singh, F.; Dole, Babasaheb. N.; Hianik, T.; Shirsat, M. D. Chemiresistive Sensor Based on Metal Organic Framework-Reduced Graphene Oxide (Cu-BTC@rGO) Nanocomposite for the Detection of Ammonia. *Eng. Proc.* **2023**, *48* (1), 32.

(34) Campbell, M. G.; Liu, S. F.; Swager, T. M.; Dincă, M. Chemiresistive Sensor Arrays from Conductive 2D Metal−Organic Frameworks. *J. Am. Chem. Soc.* **2015**, *137* (43), 13780−13783.

(35) Assfour, B.; Leoni, S.; Seifert, G. Hydrogen Adsorption Sites in Zeolite Imidazolate Frameworks ZIF-8 and ZIF-11. *J. Phys. Chem. C* **2010**, *114* (31), 13381−13384.

(36) Deacon, A.; Briquet, L.; Malankowska, M.; Massingberd-Mundy, F.; Rudić, S.; Hyde, T. l.; Cavaye, H.; Coronas, J.; Poulston, S.; Johnson, T. Understanding the ZIF-L to ZIF-8 Transformation from Fundamentals to Fully Costed Kilogram-Scale Production. *Commun. Chem.* **2022**, *5* (1), 18.

(37) Shi, Q.; Chen, Z.; Song, Z.; Li, J.; Dong, J. Synthesis of ZIF-8 and ZIF-67 by Steam-Assisted Conversion and an Investigation of Their Tribological Behaviors. *Angew. Chem., Int. Ed.* **2011**, *50* (3), 672−675.

(38) Noh, S. J.; Yoon, S. P.; Han, J.; Park, S.; Kim, J. Synthesis and Characterization of ZIF-7 Membranes by in Situ Method. *J. Nanosci. Nanotechnol.* **2015**, *15* (1), 575−578.

(39) Jafari, N.; Zeinali, S. Highly Rapid and Sensitive Formaldehyde Detection at Room Temperature Using a ZIF-8/MWCNT Nanocomposite. *ACS Omega* **2020**, *5* (9), 4395−4402.

(40) Polyakov, V. A.; Butova, V. V.; Erofeeva, E. A.; Tereshchenko, A. A.; Soldatov, A. V. MW Synthesis of ZIF-7. The Effect of Solvent on Particle Size and Hydrogen Sorption Properties. *Energies* **2020**, *13* (23), 6306.

(41) Kumari, G.; Jayaramulu, K.; Maji, T. K.; Narayana, C. Temperature Induced Structural Transformations and Gas Adsorption in the Zeolitic Imidazolate Framework ZIF-8: A Raman Study. *J. Phys. Chem. A* **2013**, *117* (43), 11006−11012.

(42) Lupan, O.; Shishiyanu, S.; Chow, L.; Shishiyanu, T. Nanostructured Zinc Oxide Gas Sensors by Successive Ionic Layer Adsorption and Reaction Method and Rapid Photothermal Processing. *Thin Solid Films* **2008**, *516* (10), 3338−3345.

(43) Lupan, O.; Chow, L.; Shishiyanu, S.; Monaico, E.; Shishiyanu, T.; Şontea, V.; Roldan Cuenya, B.; Naitabdi, A.; Park, S.; Schulte, A. Nanostructured Zinc Oxide Films Synthesized by Successive Chemical Solution Deposition for Gas Sensor Applications. *Mater. Res. Bull.* **2009**, *44* (1), 63−69.

(44) Qian, J.; Sun, F.; Qin, L. Hydrothermal Synthesis of Zeolitic Imidazolate Framework-67 (ZIF-67) Nanocrystals. *Mater. Lett.* **2012**, *82*, 220−223.

(45) Japip, S.; Xiao, Y.; Chung, T. S. Particle-Size Effects on Gas Transport Properties of 6FDA-Durene/ZIF-71 Mixed Matrix Membranes. *Ind. Eng. Chem. Res.* **2016**, *55* (35), 9507−9517.

(46) Postica, V.; Hölken, I.; Schneider, V.; Kaidas, V.; Polonskyi, O.; Cretu, V.; Tiginyanu, I.; Faupel, F.; Adelung, R.; Lupan, O. Multifunctional Device Based on ZnO:Fe Nanostructured Films with Enhanced UV and Ultra-Fast Ethanol Vapour Sensing. *Mater. Sci. Semicond. Process.* **2016**, *49*, 20−33.

(47) Nagpal, R.; Sugihara, M.; Lupan, C.; Tjardts, T.; Meling-Lizarde, N.; Strunskus, T.; Qiu, H.; Adelung, R.; Ameloot, R.; Lupan, O. ZIF-71-Coated CuO:Al with Enhanced Gas-Sensing Performance for n-Butanol and Hydrogen. *ACS Appl. Electron. Mater.* **2025**, *7* (22), 10198−10215.

(48) Soliman, A. I. A.; Abdel-Wahab, A. M. A.; Abdelhamid, H. N. Hierarchical Porous Zeolitic Imidazolate Frameworks (ZIF-8) and ZnO@N-Doped Carbon for Selective Adsorption and Photocatalytic Degradation of Organic Pollutants. *RSC Adv.* **2022**, *12* (12), 7075−7084.

(49) Dou, S.; Dong, C.; Hu, Z.; Huang, Y.; Chen, J.; Tao, L.; Yan, D.; Chen, D.; Shen, S.; Chou, S.; Wang, S. Atomic-Scale CoOx

Species in Metal−Organic Frameworks for Oxygen Evolution Reaction. *Adv. Funct. Mater.* **2017**, *27* (36), No. 1702546.
(50) Joshi, B. N.; Lee, J.-G.; An, S.; Kim, D.-Y.; Lee, J. S.; Hwang, Y. K.; Chang, J.-S.; Al-Deyab, S. S.; Tan, J.-C.; Yoon, S. S. Tuning Crystalline Structure of Zeolitic Metal−Organic Frameworks by Supersonic Spraying of Precursor Nanoparticle Suspensions. *Mater. Des.* **2017**, *114*, 416−423.
(51) Thi Thanh, M.; Vinh Thien, T.; Thi Thanh Chau, V.; Dinh Du, P.; Phi Hung, N.; Quang Khieu, D. Synthesis of Iron Doped Zeolite Imidazolate Framework-8 and Its Remazol Deep Black RGB Dye Adsorption Ability. *J. Chem.* **2017**, *2017* (1), No. 5045973.
(52) Feng, X.; Carreon, M. A. Kinetics of Transformation on ZIF-67 Crystals. *J. Cryst. Growth* **2015**, *418*, 158−162.
(53) Banerjee, R.; Phan, A.; Wang, B.; Knobler, C.; Furukawa, H.; O'Keeffe, M.; Yaghi, O. M. High-Throughput Synthesis of Zeolitic Imidazolate Frameworks and Application to CO_2 Capture. *Science* **2008**, *319* (5865), 939−943.
(54) Vigil, O.; Vaillant, L.; Cruz, F.; Santana, G.; Morales-Acevedo, A.; Contreras-Puente, G. Spray Pyrolysis Deposition of Cadmium−Zinc Oxide Thin Films. *Thin Solid Films* **2000**, *361*, 53−55.
(55) Lupan, O.; Pauporté, T.; Le Bahers, T.; Ciofini, I.; Viana, B. High Aspect Ratio Ternary $Zn_{1-X}Cd_xO$ Nanowires by Electrodeposition for Light-Emitting Diode Applications. *J. Phys. Chem. C* **2011**, *115* (30), 14548−14558.
(56) Sharma, S.; Chand, P. Electrochemical Behavior of Solvothermally Grown ZIF-8 as Electrode Material for Supercapacitor Applications. *Mater. Today Proc.* **2023**, *76*, 125−131.
(57) Dubrovkin, Joseph*Data Compression in Spectroscopy*; Cambridge Scholars Publishing, 2022.
(58) Olivero, J. J.; Longbothum, R. L. Empirical Fits to the Voigt Line Width: A Brief Review. *J. Quant. Spectrosc. Radiat. Transfer* **1977**, *17* (2), 233−236.
(59) Samanta, P. K. Effect of Microstrain on the Crystallite Size of ZnO Nanoparticles: X-Ray Peak Profile and Rietveld Analysis. *Next Materials* **2025**, *8*, No. 100841.
(60) Byrne, C.; Mazaj, M.; Logar, N. Z. Assessing the Heat Storage Potential of Zeolitic Imidazolate Frameworks (ZIFs) Using Water and Ethanol as Working Fluids. *Mater. Chem. Phys.* **2025**, *332*, No. 130143.
(61) Pelka, R.; Arabczyk, W. A New Method for Determining the Nanocrystallite Size Distribution in Systems Where Chemical Reaction between Solid and a Gas Phase Occurs. *J. Nanomater.* **2013**, *2013*, No. 645050.
(62) Coudert, F.-X. Responsive Metal−Organic Frameworks and Framework Materials: Under Pressure, Taking the Heat, in the Spotlight, with Friends. *Chem. Mater.* **2015**, *27* (6), 1905−1916.
(63) Zhao, P.; Lampronti, G. I.; Lloyd, G. O.; Wharmby, M. T.; Facq, S.; Cheetham, A. K.; Redfern, S. A. T. Phase Transitions in Zeolitic Imidazolate Framework 7: The Importance of Framework Flexibility and Guest-Induced Instability. *Chem. Mater.* **2014**, *26* (5), 1767−1769.
(64) Kannaka, S.; Ohmiya, A.; Ozaki, C.; Ohtani, M. Thermodynamic Analysis of Gate-Opening Carbon Dioxide Adsorption Behavior of Metal−Organic Frameworks. *Chem. Commun.* **2024**, *60* (31), 4170−4173.
(65) James, J. B.; Lin, Y. S. Kinetics of ZIF-8 Thermal Decomposition in Inert, Oxidizing, and Reducing Environments. *J. Phys. Chem. C* **2016**, *120* (26), 14015−14026.
(66) Chen, S.; Li, X.; Dong, E.; Lv, H.; Yang, X.; Liu, R.; Liu, B. Intrinsic and Extrinsic Responses of ZIF-8 under High Pressure: A Combined Raman and X-Ray Diffraction Investigation. *J. Phys. Chem. C* **2019**, *123* (49), 29693−29707.
(67) Hao, J.; Babu, D. J.; Liu, Q.; Schouwink, P. A.; Asgari, M.; Queen, W. L.; Agrawal, K. V. Mechanistic Study on Thermally Induced Lattice Stiffening of ZIF-8. *Chem. Mater.* **2021**, *33* (11), 4035−4044.
(68) Frentzel-Beyme, L.; Kloß, M.; Pallach, R.; Salamon, S.; Moldenhauer, H.; Landers, J.; Wende, H.; Debus, J.; Henke, S. Porous Purple Glass − a Cobalt Imidazolate Glass with Accessible Porosity from a Meltable Cobalt Imidazolate Framework. *J. Mater. Chem. A* **2019**, *7* (3), 985−990.
(69) Guzmán-Embús, D. A.; Vargas-Charry, M. F.; Vargas-Hernández, C. Optical and Structural Properties of ZnO and ZnO:Cd Particles Grown by the Hydrothermal Method. *J. Am. Ceram. Soc.* **2015**, *98* (5), 1498−1505.
(70) Cuscó, R.; Alarcón-Lladó, E.; Ibáñez, J.; Artús, L.; Jiménez, J.; Wang, B.; Callahan, M. J. Temperature dependence of Raman scattering in ZnO. *Phys. Rev. B* **2007**, *75* (16), No. 165202.
(71) Torchynska, T.; El Filali, B.; Jaramillo Gomez, J. A.; Polupan, G.; Ramírez García, J. L.; Shcherbyna, L. Raman Scattering, Emission, and Deep Defect Evolution in ZnO:In Thin Films. *J. Vac. Sci. Technol., A* **2020**, *38* (6), No. 063409.
(72) Nizar, B. M.; Lajnef, M.; Chaste, J.; Chtourou, R.; Herth, E. Highly C-Oriented (002) Plane ZnO Nanowires Synthesis. *RSC Adv.* **2023**, *13* (22), 15077−15085.
(73) Sahoo, S.; Sharma, G. L.; Katiyar, R. S. Raman Spectroscopy to Probe Residual Stress in ZnO Nanowire. *J. Raman Spectrosc.* **2012**, *43* (1), 72−75.
(74) Stanković, A.; Stojanović, Z.; Veselinović, L.; Škapin, S. D.; Bračko, I.; Marković, S.; Uskoković, D. ZnO Micro and Nanocrystals with Enhanced Visible Light Absorption. *Mater. Sci. Eng., B* **2012**, *177* (13), 1038−1045.
(75) Narimbi, J.; Balakrishnan, S.; Perova, T. S.; Dee, G.; Swiegers, G. F.; Gun'ko, Y. K. XRD and Spectroscopic Investigations of ZIF—Microchannel Glass Plates Composites. *Materials* **2023**, *16* (6), 2410.
(76) Cai, X.; Peng, F.; Luo, X.; Ye, X.; Zhou, J.; Lang, X.; Shi, M. Understanding the Evolution of Cobalt-Based Metal-Organic Frameworks in Electrocatalysis for the Oxygen Evolution Reaction. *ChemSusChem* **2021**, *14* (15), 3163−3173.
(77) Júnior, E. A. A.; Nobre, F. X.; da Silva Sousa, G.; Cavalcante, L. S.; Santos, M. R. D. M. C.; Souza, F. L.; de Matos, J. M. E. Synthesis, Growth Mechanism, Optical Properties and Catalytic Activity of ZnO Microcrystals Obtained via Hydrothermal Processing. *RSC Adv.* **2017**, *7* (39), 24263−24281.
(78) Ouni, B.; Larbi, T.; Amlouk, M. Vibrational, Electronic and Structural Study of Sprayed ZnO Thin Film Based on the IR-Raman Spectra and DFT Calculations. *Cryst. Struct. Theory Appl.* **2022**, *11* (02), 23−38.
(79) Sun, Y.; Li, Y.; Tan, J. C. Liquid Intrusion into Zeolitic Imidazolate Framework-7 Nanocrystals: Exposing the Roles of Phase Transition and Gate Opening to Enable Energy Absorption Applications. *ACS Appl. Mater. Interfaces* **2018**, *10* (48), 41831−41838.
(80) Möslein, A. F.; Tan, J. C. Vibrational Modes and Terahertz Phenomena of the Large-Cage Zeolitic Imidazolate Framework-71. *J. Phys. Chem. Lett.* **2022**, *13* (12), 2838−2844.
(81) Ye, J.; Tan, J. C.; Ye, J.; Tan, J. High-Performance Triboelectric Nanogenerators Incorporating Chlorinated Zeolitic Imidazolate Frameworks with Topologically Tunable Dielectric and Surface Adhesion Properties. *Nano Energy* **2023**, *114*, No. 108687.
(82) Zhang, Y.; Gutiérrez, M.; Chaudhari, A. K.; Tan, J.-C. Dye-Encapsulated Zeolitic Imidazolate Framework (ZIF-71) for Fluorochromic Sensing of Pressure, Temperature, and Volatile Solvents. *ACS Appl. Mater. Interfaces* **2020**, *12* (33), 37477−37488.
(83) Mollick, S.; Zhang, Y.; Kamal, W.; Tricarico, M.; Möslein, A. F.; Kachwal, V.; Amin, N.; Castrejón-Pita, A. A.; Morris, S. M.; Tan, J.-C.Surface Modulation of Metal-Organic Frameworks for on-Demand Photochromism in the Solid State, *Arxiv*, **2022**, .
(84) Olaniyan, B.; Saha, B. Comparison of Catalytic Activity of ZIF-8 and Zr/ZIF-8 for Greener Synthesis of Chloromethyl Ethylene Carbonate by CO2 Utilization. *Energies* **2020**, *13* (3), 521.
(85) Li, J.; Chang, H.; Li, Y.; Li, Q.; Shen, K.; Yi, H.; Zhang, J. Synthesis and Adsorption Performance of La@ZIF-8 Composite Metal−Organic Frameworks. *RSC Adv.* **2020**, *10* (6), 3380−3390.
(86) Hu, H.; Liu, S.; Chen, C.; Wang, J.; Zou, Y.; Lin, L.; Yao, S. Two Novel Zeolitic Imidazolate Frameworks (ZIFs) as Sorbents for Solid-Phase Extraction (SPE) of Polycyclic Aromatic Hydrocarbons

(PAHs) in Environmental Water Samples. *Analyst* **2014**, *139* (22), 5818−5826.
(87) Martínez-Salazar, M.; Tiempos Flores, N.; Obregón-Zúñiga, A.; Arillo-Flores, O. I.; Dávila-Guzmán, N. E.; Michaelis, D. J.; Raziel Álvarez, J.; Hernández-Fernández, E. Dye Removal Utilizing ZIF-71 and Hydrophobic ZIF-71(ClBr): Kinetic and Equilibrium Studies. *ACS Omega* **2025**, *10* (38), 43404−43414.
(88) Bergaoui, M.; Khalfaoui, M.; Awadallah-F, A.; Al-Muhtaseb, S. A Review of the Features and Applications of ZIF-8 and Its Derivatives for Separating CO_2 and Isomers of C3- and C4-Hydrocarbons. *J. Nat. Gas Sci. Eng.* **2021**, *96*, No. 104289.
(89) Malepe, L.; Ndinteh, T. D.; Ndungu, P.; Mamo, M. A. A Humidity Tolerance and Room Temperature Carbon Soot@ZIF-71 Sensor for Toluene Vapour Detection. *Mater. Res. Bull.* **2025**, *181*, No. 113076.
(90) Yang, X.; Jiang, S.; Zhang, Z.; Li, B.; Xu, M. The Preparation of ZIF-67 and Its Synergistic Effect on Fire Performance of Intumescent Flame Retardant Polypropylene. *J. Therm. Anal. Calorim.* **2023**, *148* (18), 9547−9560.
(91) Sun, M.; Wang, M.; Ge, C.; Huang, J.; Li, Y.; Yan, P.; Wang, M.; Lei, S.; Bai, L.; Qiao, G. Au-Doped ZnO@ZIF-7 Core-Shell Nanorod Arrays for Highly Sensitive and Selective NO2 Detection. *Sens. Actuators, B* **2023**, *384*, No. 133632.
(92) Tu, M.; Xia, B.; Kravchenko, D. E.; Tietze, M. L.; Cruz, A. J.; Stassen, I.; Hauffman, T.; Teyssandier, J.; De Feyter, S.; Wang, Z.; Fischer, R. A.; Marmiroli, B.; Amenitsch, H.; Torvisco, A.; Velásquez-Hernández, M. de J.; Falcaro, P.; Ameloot, R. Direct X-Ray and Electron-Beam Lithography of Halogenated Zeolitic Imidazolate Frameworks. *Nat. Mater.* **2021**, *20* (1), 93−99.
(93) Li, W.; Ma, T.; Tang, P.; Luo, Y.; Zhang, H.; Zhao, J.; Ameloot, R.; Tu, M. Nanoscale Resist-Free Patterning of Halogenated Zeolitic Imidazolate Frameworks by Extreme UV Lithography. *Advanced Science* **2025**, *12* (16), No. 2415804.
(94) Tian, F.; Cerro, A. M.; Mosier, A. M.; Wayment-Steele, H. K.; Shine, R. S.; Park, A.; Webster, E. R.; Johnson, L. E.; Johal, M. S.; Benz, L. Surface and Stability Characterization of a Nanoporous ZIF-8 Thin Film. *J. Phys. Chem. C* **2014**, *118* (26), 14449−14456.
(95) Li, Y.; Wee, L. H.; Martens, J. A.; Vankelecom, I. F. J. ZIF-71 as a Potential Filler to Prepare Pervaporation Membranes for Bio-Alcohol Recovery. *J. Mater. Chem. A* **2014**, *2* (26), 10034−10040.
(96) Schweinefuß, M. E.; Springer, S.; Baburin, I. A.; Hikov, T.; Huber, K.; Leoni, S.; Wiebcke, M. Zeolitic Imidazolate Framework-71 Nanocrystals and a Novel SOD-Type Polymorph: Solution Mediated Phase Transformations, Phase Selection via Coordination Modulation and a Density Functional Theory Derived Energy Landscape. *Dalton Trans.* **2014**, *43* (9), 3528−3536.
(97) Lively, R. P.; Dose, M. E.; Thompson, J. A.; McCool, B. A.; Chance, R. R.; Koros, W. J. Ethanol and Water Adsorption in Methanol-Derived ZIF-71. *Chem. Commun.* **2011**, *47* (30), 8667−8669.
(98) Mtangi, W.; Auret, F. D.; Nyamhere, C.; Janse van Rensburg, P. J.; Chawanda, A.; Diale, M.; Nel, J. M.; Meyer, W. E. The Dependence of Barrier Height on Temperature for Pd Schottky Contacts on ZnO. *Phys. B: Condens. Matter* **2009**, *404* (22), 4402−4405.
(99) Bisquert, J. Inductive and Capacitive Hysteresis of Current-Voltage Curves: Unified Structural Dynamics in Solar Energy Devices, Memristors, Ionic Transistors, and Bioelectronics. *PRX Energy* **2024**, *3* (1), No. 011001.
(100) Bisquert, J.; Guerrero, A.; Gonzales, C. Theory of Hysteresis in Halide Perovskites by Integration of the Equivalent Circuit. *ACS Phys. Chem. Au* **2021**, *1* (1), 25−44.
(101) Rathnasekara, R.; Mayberry, G. M.; Hari, P. Deep-Level Transient Spectroscopy Studies on Four Different Zinc Oxide Morphologies. *Crystals* **2024**, *14* (3), 224.
(102) Zhao, X.; Li, J.; Li, H.; Li, S. Intrinsic and Extrinsic Defect Relaxation Behavior of ZnO Ceramics. *J. Appl. Phys.* **2012**, *111* (12), No. 124106.
(103) Patwari, G.; Kalita, P. K.; Singha, R. Structural and Optoelectronic Properties of Glucose Capped Al and Cu Doped ZnO Nanostructures. *Mater. Sci.-Pol.* **2016**, *34* (1), 69−78.
(104) Elhamdi, I.; Souissi, H.; Taktak, O.; Elghoul, J.; Kammoun, S.; Dhahri, E.; Costa, B. F. O. Experimental and Modeling Study of ZnO:Ni Nanoparticles for near-Infrared Light Emitting Diodes. *RSC Adv.* **2022**, *12* (21), 13074−13086.
(105) Kortidis, I.; Lushozi, S.; Leshabane, N.; Nkosi, S. S.; Ndwandwe, O. M.; Tshilongo, J.; Ntsasa, N.; Motaung, D. E. Selective Detection of Propanol Vapour at Low Operating Temperature Utilizing ZnO Nanostructures. *Ceram. Int.* **2019**, *45* (13), 16417−16423.
(106) Huang, H.; Du, Z.; Wu, H.-C.; Gao, F.; Jiang, L.; Hou, H.; Chen, S.; Li, W.; Hu, F.; Yang, W.; Zhang, D.; Wang, L. High-Temperature Resistant Ethanol Sensing Enhanced by ZnO Nanoparticles/SiC Nanowire Heterojunctions. *Appl. Surf. Sci.* **2024**, *645*, No. 158828.
(107) Piliai, L.; Tomeček, D.; Hruška, M.; Khalakhan, I.; Nováková, J.; Fitl, P.; Yatskiv, R.; Grym, J.; Vorokhta, M.; Matolínová, I.; Vrňata, M. New Insights towards High-Temperature Ethanol-Sensing Mechanism of ZnO-Based Chemiresistors. *Sensors* **2020**, *20* (19), 5602.
(108) Meng, F.; Li, G.; Ji, H.; Yuan, Z. Investigation on Oxygen Vacancy Regulation Mechanism of ZnO Gas Sensors under Temperature Modulation Mode to Distinguish Alcohol Homologue Gases. *Sens. Actuators, B* **2025**, *423*, No. 136747.
(109) Yang, X.; Wang, W.; Xiong, J.; Chen, L.; Ma, Y. ZnO:Cd Nanorods Hydrogen Sensor with Low Operating Temperature. *Int. J. Hydrogen Energy* **2015**, *40* (36), 12604−12609.
(110) Liu, X.; Chen, N.; Xing, X.; Li, Y.; Xiao, X.; Wang, Y.; Djerdj, I. A High-Performance n-Butanol Gas Sensor Based on ZnO Nanoparticles Synthesized by a Low-Temperature Solvothermal Route. *RSC Adv.* **2015**, *5* (67), 54372−54378.
(111) Rout, C. S.; Hari Krishna, S.; Vivekchand, S. R. C.; Govindaraj, A.; Rao, C. N. R. Hydrogen and Ethanol Sensors Based on ZnO Nanorods, Nanowires and Nanotubes. *Chem. Phys. Lett.* **2006**, *418* (4), 586−590.
(112) Hazra, S. K.; Basu, S. Hydrogen Sensitivity of ZnO p−n Homojunctions. *Sens. Actuators, B* **2006**, *117* (1), 177−182.
(113) Park, S. High-Response and Selective Hydrogen Sensing Properties of Porous ZnO Nanotubes. *Curr. Appl. Phys.* **2016**, *16* (10), 1263−1269.
(114) Zhao, R.; Li, K.; Wang, Z.; Xing, X.; Wang, Y. Gas-Sensing Performances of Cd-Doped ZnO Nanoparticles Synthesized by a Surfactant-Mediated Method for n-Butanol Gas. *J. Phys. Chem. Solids* **2018**, *112*, 43−49.
(115) Momma, K.; Izumi, F. VESTA 3 for Three-Dimensional Visualization of Crystal, Volumetric and Morphology Data. *J. Appl. Crystallogr.* **2011**, *44* (6), 1272−1276.
(116) Jones, I. M.; Turner, G. F.; Pitts, K.; Powell, R.; Riboldi-Tunnicliffe, A.; Williamson, R.; Boer, S.; Allen, L.; Moggach, S. A. High-Pressure Induced Guest-Mediated Gate Opening Behaviour of the Co-Based Framework ZIF-67. *CrystEngComm* **2023**, *25* (47), 6533−6538.
(117) Derouane, E. G. The Energetics of Sorption by Molecular Sieves: Surface Curvature Effects. *Chem. Phys. Lett.* **1987**, *142* (3), 200−204.
(118) Hu, H.; Zhu, J.; Yang, F.; Chen, Z.; Deng, M.; Weng, L.; Ling, Y.; Zhou, Y. A Robust Etb-Type Metal−Organic Framework Showing Polarity-Exclusive Adsorption of Acetone over Methanol for Their Azeotropic Mixture. *Chem. Commun.* **2019**, *55* (46), 6495−6498.
(119) Gao, C.; Shi, Q.; Dong, J. Adsorptive Separation Performance of 1-Butanol onto Typical Hydrophobic Zeolitic Imidazolate Frameworks (ZIFs). *CrystEngComm* **2016**, *18* (21), 3842−3849.
(120) Tuan, V. A.; Li, S.; Falconer, J. L.; Noble, R. D. In Situ Crystallization of Beta Zeolite Membranes and Their Permeation and Separation Properties. *Chem. Mater.* **2002**, *14* (2), 489−492.
(121) Xiong, Y.; Xu, W.; Zhu, Z.; Xue, Q.; Lu, W.; Ding, D.; Zhu, L. ZIF-Derived Porous ZnO-Co3O4 Hollow Polyhedrons Heterostruc-

ture with Highly Enhanced Ethanol Detection Performance. *Sens. Actuators, B* **2017**, *253*, 523−532.

(122) Altun, B.; Karaduman Er, I.; Çağırtekin, A. O.; Ajjaq, A.; Sarf, F.; Acar, S. Effect of Cd Dopant on Structural, Optical and CO_2 Gas Sensing Properties of ZnO Thin Film Sensors Fabricated by Chemical Bath Deposition Method. *Appl. Phys. A* **2021**, *127* (9), 687.

(123) Du, Y.; Wooler, B.; Nines, M.; Kortunov, P.; Paur, C. S.; Zengel, J.; Weston, S. C.; Ravikovitch, P. I. New High- and Low-Temperature Phase Changes of ZIF-7: Elucidation and Prediction of the Thermodynamics of Transitions. *J. Am. Chem. Soc.* **2015**, *137* (42), 13603−13611.

(124) Lupan, O.; Chow, L.; Pauporté, Th.; Ono, L. K.; Roldan Cuenya, B.; Chai, G. Highly Sensitive and Selective Hydrogen Single-Nanowire Nanosensor. *Sens. Actuators, B* **2012**, *173*, 772−780.

(125) Vandezande, W.; Janssen, K. P. F.; Delport, F.; Ameloot, R.; De Vos, D. E.; Lammertyn, J.; Roeffaers, M. B. J. Parts per Million Detection of Alcohol Vapors via Metal Organic Framework Functionalized Surface Plasmon Resonance Sensors. *Anal. Chem.* **2017**, *89* (8), 4480−4487.

(126) Wei, K.; Zhao, S.; Zhang, W.; Zhong, X.; Li, T.; Cui, B.; Gao, S.; Wei, D.; Shen, Y. Controllable Synthesis of Zn-Doped α-Fe2O3 Nanowires for H2S Sensing. *Nanomaterials* **2019**, *9* (7), 994.

(127) Schlaich, A.; Barrat, J. L.; Coasne, B. Theory and Modeling of Transport for Simple Fluids in Nanoporous Materials: From Microscopic to Coarse-Grained Descriptions. *Chem. Rev.* **2025**, *125*, 2561−2624.

(128) Nagpal, Rajat; Ababii, N.; Lupan, O. Comprehensive Advances in Gas Sensing: Mechanisms, Material Innovations, and Applications in Environmental and Health Monitoring. *Mater. Today Electron.* **2025**, No. 100192.

(129) Chowdhury, N. K.; Bhowmik, B. Micro/Nanostructured Gas Sensors: The Physics behind the Nanostructure Growth, Sensing and Selectivity Mechanisms. *Nanoscale Adv.* **2021**, *3* (1), 73−93.

(130) Mokoena, T. P.; Swart, H. C.; Hillie, K. T.; Tshabalala, Z. P.; Jozela, M.; Tshilongo, J.; Motaung, D. E. Enhanced Propanol Gas Sensing Performance of P-Type NiO Gas Sensor Induced by Exceptionally Large Surface Area and Crystallinity. *Appl. Surf. Sci.* **2022**, *571*, No. 151121.

(131) Chowdhury, N. K.; Bhowmik, B. Pd/TiO2 Nanosheet/Ti Sensor towards Propanol Sensing: Influence of Edge Energy and Defect States. *Mater. Today Proc.* **2022**, *56*, 984−988.

(132) Wang, J.; Yang, J.; Han, N.; Zhou, X.; Gong, S.; Yang, J.; Hu, P.; Chen, Y. Highly Sensitive and Selective Ethanol and Acetone Gas Sensors Based on Modified ZnO Nanomaterials. *Mater. Des.* **2017**, *121*, 69−76.

(133) Choudhary, M.; Shrivastav, A.; Sinha, A. K.; Chawla, A. K.; Avasthi, D. K.; Saravanan, K.; Krishnamurthy, S.; Chandra, R.; Wadhwa, S. Emerging Nanomaterials for Hydrogen Sensing: Mechanisms and Prospects. *Int. J. Hydrogen Energy* **2024**, *77*, 557−574.

(134) Kim, H.-J.; Lee, J.-H. Highly Sensitive and Selective Gas Sensors Using P-Type Oxide Semiconductors: Overview. *Sens. Actuators, B* **2014**, *192*, 607−627.

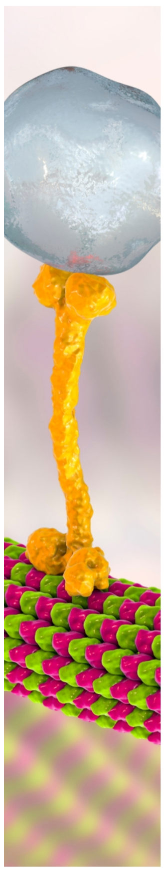

https://doi.org/10.1021/acsomega.6c02238
ACS Omega 2026, 11, 29178−29201